

1. Methods: Description of the climate model LOVECLIM

LOVECLIM consists of five components representing the atmosphere (ECBilt), the ocean and sea ice (CLIO), the terrestrial biosphere (VECODE), the oceanic carbon cycle (LOCH) and the Greenland and Antarctic ice sheets (AGISM). ECBilt is a quasi-geostrophic atmospheric model with 3 levels and a T21 horizontal resolution (Opsteegh et al. 1998), which contains a full hydrological cycle and explicitly computes synoptic variability associated with weather patterns. Cloud cover is prescribed according to present-day climatology, which is a limitation of the present study. CLIO is a primitive-equation, free-surface ocean general circulation model coupled to a thermodynamic-dynamic sea-ice model (Goosse and Fichefet 1999). Its horizontal resolution is $3^\circ \times 3^\circ$, and there are 20 levels in the ocean. VECODE is a reduced-form model of vegetation dynamics and of the terrestrial carbon cycle (Brovkin et al. 2002). It simulates the dynamics of two plant functional types (trees and grassland) at the same resolution as that of ECBilt. ECBilt-CLIO-VECODE has been utilized in a large number of climate studies (please refer to <http://www.knmi.nl/onderzk/CKO/ecbilt-papers.html> for a full list of references). LOCH is a comprehensive model of the oceanic carbon cycle (Mouchet and Francois 1996). It takes into account both the solubility and biological pumps, and runs on the same grid as the one of CLIO. This model was not activated in the present study, and we prescribe the evolution of the atmospheric CO_2 concentration. Finally, AGISM is composed of two three-dimensional thermomechanical models of the ice-sheet flow, coupled to a visco-elastic bedrock model and a model of the mass balance at the ice-atmosphere and ice-ocean interfaces (Huybrechts 2002). For both ice sheets, calculations are made on a $10 \text{ km} \times 10 \text{ km}$ resolution grid with 31 sigma levels. Given the long time-scales investigated here, the model is among the most complex climate models that can be applied to study this type of questions at present. Note that the mask of the ice shelves is fixed under present-day configuration, and the land-sea mask is not modified during the integration for the ocean, but can change for the ice-sheet models.

The atmospheric variables needed as input for AGISM are surface temperature and precipitation. Because the details of the Greenland and Antarctica surface climates are not well captured on the ECBilt coarse grid, these boundary conditions consist of present-day observations as represented on the much finer AGISM grid onto which climate change anomalies from ECBilt are superimposed (Driesschaert et al. 2007). Monthly temperature differences and annual precipitation ratios, computed against a reference climate corresponding to the period 1970-2000 AD, are interpolated from the ECBilt grid onto the AGISM grid and added to and multiplied by the observed surface temperatures and precipitation rates, respectively. The oceanic heat flux at the base of Antarctic ice shelves is also calculated in perturbation mode using the parameterization proposed by Beckmann and Goosse

(2003). After performing mass balance and ice dynamics computations, AGISM transmits the calculated changes in land fraction covered by ice and in orography to EC-Bilt and VECODE. In addition, AGISM provides CLIO with the geographical distribution of the annual mean surface freshwater flux resulting from ice sheet runoff, iceberg calving, runoff from ice-free land and basal ice melting from both below the grounded ice sheet and its surrounding ice shelves. All of these sources of fresh water are added to the surface layer of coastal oceanic grid boxes. The Greenland (Antarctic) ice-sheet module was first integrated over the last two (four) glacial cycles up to 1500 AD with forcing from ice core data to derive initial conditions for coupling with the other components of LOVECLIM. The control experiment (CTRL) of 3000-year duration was then conducted with LOVECLIM under forcing conditions corresponding to 1500 AD. The same initial conditions are used for all the scenario simulations performed in this study.

The model version used here is LOVECLIM1.1. Three main improvements have been incorporated in this version compared to LOVECLIM1.0 (Goosse et al. 2007). First, the land-surface scheme has been modified (see http://www.astr.ucl.ac.be/ASTER/doc/E_AR_SDCS01A_v2.pdf) in order to take into account the impact of the changes in vegetation on the evaporation (transpiration) and on the bucket depth (i.e. the maximum water that can be hold in the soil). Second, the emissivity, which was the same for all the surface types in LOVECLIM1.0, is now different for land, ocean and sea ice. Third, in order to reduce the artificial vertical diffusion in the ocean caused by numerical noise, the Coriolis term is now treated in a fully implicit way in the equation of motion for the ocean, while a semi-implicit scheme was used in LOVECLIM1.0.

2. Supplementary discussion 1: Mass balance of the Antarctic ice sheet

Under global warming conditions, the mass balance of the grounded AIS depends on the rate of change in accumulation over the ice sheet and ice loss around its perimeter, through surface runoff and ice discharge across the grounding line into the surrounding ice shelves. Few studies have analysed the long-term mass balance of the AIS in millennial projections. Huybrechts and De Wolde (1999) find a negative sea-level rise contribution from the AIS of -0.3 m after 1000 years in a $4\times\text{CO}_2$ experiment similar to the one performed in the present study, but with the forcing derived from a two-dimensional climate model. An annual mean temperature rise over Antarctica of 5.5°C is simulated in the Huybrechts and De Wolde (1999) study after 1000 years. In an $8\times\text{CO}_2$ experiment, Huybrechts and De Wolde (1999) simulate an 8.5°C warming over Antarctica and a positive sea-level rise contribution of 0.8 m after 1000 years. More recently, Mikolajewicz et al. (2007), using another ice-sheet model coupled to a state-of-the-art climate model, find negative contribution in terms of sea-level rise for the AIS in different projections using emission scenarios going from B1 up to A2. In their model the increase in accumulation over the grounded AIS is always larger than the increase in ablation for the grounded AIS.

In the present study, the simulated warming over Antarctica after 3000 years is rather large in the projections as compared to CTRL. The annual mean temperature rise over Antarctica reaches values of 9°C in iAiG and 12°C in fAfG for a spatial average over Antarc-

tica. This is due to a large polar amplification in this model that leads to an important warming over the AIS in fAfG (Supplementary Figure 1.b). This polar amplification put the model used here in the higher range of polar amplification as simulated in climate models (Meehl et al. 2007, Masson-Delmotte et al. 2006). Nonetheless, since this model is on the lower range for climate sensitivity (Meehl et al. 2007), the simulated warming over the AIS is not unrealistic, given the several centuries necessary to reach such a warming, due to the thermal inertia of the Southern Ocean. This large warming over the AIS leads to a rather rapid decay of the West AIS in fAfG and also a substantial retreat in some coastal parts of the East AIS, notably in the Ninnis-Mertz glacier basins in Victoria Land (Supplementary Figure 4). The processes causing this decay are both the development of a peripheral surface ablation zone, as in Greenland today, as the demise of the surrounding ice shelves from both large increases in surface and bottom melting. Consequently, the grounded AIS already loses a substantial fraction of its mass after 1000 years in iAiG and fAfG (Supplementary Figure 2), due to a larger increase of ablation (sum of surface runoff from grounded ice, basal melting below grounded ice, flux across grounding line) over accumulation (Supplementary Figure 1.a). The AIS melting corresponds here, after 1000 years, to a sea-level rise of 0.5 m in iAiG and 1.5 m in fAfG. This result differs from Huybrechts and De Wolde (1999) for a $4\times\text{CO}_2$ experiment, but is coherent with the AIS response to a larger warming as found in the $8\times\text{CO}_2$ experiment, in which the warming over Antarctica in Huybrechts and De Wolde (1999) is similar to our $4\times\text{CO}_2$ experiment. The differences in mass balance response of the AIS compared to the Huybrechts and De Wolde (1999) and Mikolajewicz et al. (2007) are therefore due to the different climate model used here that exhibits a large polar amplification and warming over Antarctica.

3. Supplementary discussion 2: Issues concerning the bi-polar ocean seesaw

The effect of the bi-polar ocean seesaw has been illustrated in numerical simulations (Stocker et al. 1992, Seidov et al. 2001) and it has been shown that changing surface buoyancy forcing in key deep-water formation areas can disturb the balance between NADW and AABW cells on millennial time-scales. Thus a decrease in AABW formation reduces the AABW cell and enhances the NADW cell. The exact oceanic mechanism that yields this interaction however remains unclear. Furthermore, recent simulations (Stouffer et al. 2007, Seidov et al. 2005) show that, on centennial time-scales, an additional 1 Sv input of freshwater into the ocean, south of 60°S , has nearly no impact on the NADW cell. This result questions the validity of the bi-polar ocean seesaw since AABW formation is strongly reduced in those experiments. Two explanations arise to account for this issue: (i) the Seidov et al. (2005) and Stouffer et al. (2007) experiments use transient simulations and the bi-polar ocean seesaw effect applies on longer time-scales, due to adjustment in the ocean interior that necessitates thousands of years; (ii) the experimental design of the numerical simulations from Stocker et al. (1992) and Seidov et al. (2001) on the one side, and Seidov et al. (2005) and Stouffer et al. (2007) on the other side, are different since the first-named impose surface buoyancy forcing anomalies in some key regions of the Southern Ocean, using an

ocean-only model, while the last-named, using an ocean-atmosphere coupled model, put freshwater anomalies in the ocean south of 60°S , which can spread through the intense currents of the Southern Ocean.

In the present study, we have shown that even with an experimental design where freshwater is released into the ocean, using a coupled climate model, the bi-polar ocean seesaw applies in LOVECLIM. We propose to analyze in further depth the exact mechanisms of the bi-polar ocean seesaw in a future study, since it is not the focus of the present one, in order to try piecing some of the puzzle together.

References

- Beckmann, A., and H. Goosse (2003), A parameterization of ice shelf-ocean interaction for climate models, *Ocean Modell.*, *5*, 157–170.
- Brovkin, V., et al. (2002), Carbon cycle, vegetation, and climate dynamics in the Holocene: Experiments with the CLIMBER-2 model. *Global Biogeochem. Cycles*, *16*, doi:10.1029/2001GB001662.
- Goosse, H., and T. Fichefet (1999), Importance of ice-ocean interactions for the global ocean circulation: A model study, *J. Geophys. Res.*, *104*, 337–355.
- Goosse, H., E. Driesschaert, T. Fichefet, and M.-F. Loutre (2007), Information on the early Holocene climate constrains the summer sea ice projections for the 21st century. In press in *Climate of the Past Discussion*.
- Huybrechts, P., and J. de Wolde (1999), The dynamic response of the Greenland and Antarctic ice sheets to multiple-century climatic warming. *J. Climate*, *12*, 2169–2188.
- Huybrechts, P., (2002), Sea-level changes at the LGM from ice-dynamic reconstructions of the Greenland and Antarctic ice sheets during the glacial cycles. *Quat. Sci. Rev.*, *21*, 203–231.
- Masson-Delmotte, V., et al. (2006), Past and future polar amplification of climate change: climate model intercomparisons and ice-core constraints, *Clim. Dyn.*, *27*, 437–440.
- Mouchet, A., and L. M. Francois (1996), Sensitivity of a global oceanic carbon cycle model to the circulation and to the fate of organic matter: Preliminary results. *Phys. Chem. Earth*, *21*, 511–516.
- Opsteegh, J. D., et al. (1998), ECBILT: A dynamic alternative to mixed boundary conditions in ocean models. *Tellus A*, *50*, 348–367.
- Seidov, D., R. J. Stouffer, and B. J. Haupt (2005), Is there a simple bi-polar ocean seesaw? *Global Planetary Change*, *49*, 19–27.
-

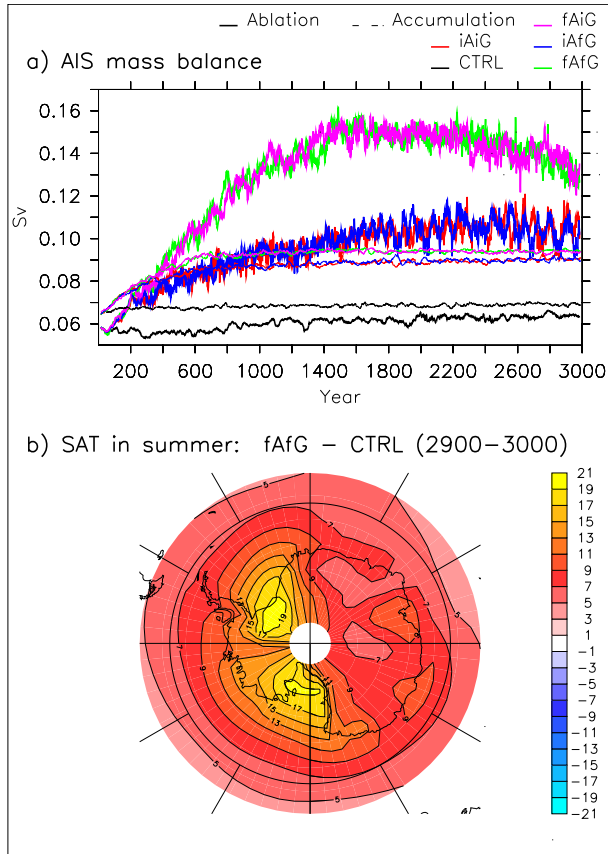


Figure 1. a) Time series of the annual mean ablation (sum of surface runoff from grounded ice, basal melting below grounded ice, flux across grounding line, represented in thick line) and accumulation (in dash line) expressed in Sv for the grounded AIS from CTRL (black), iAiG (red), fAfG (green), iAfG (blue) and fAiG (purple). b) SAT difference in austral summer (December-January-February-March) between fAfG and CTRL, averaged over years 2900 to 3000. The contour interval is 2°C.

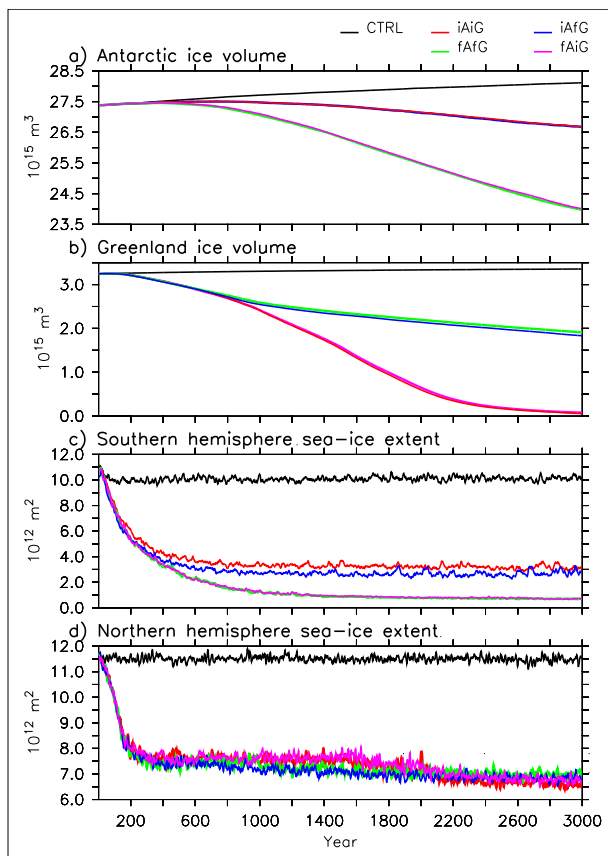


Figure 2. Time series of the annual mean cryospheric changes from CTRL (black), iAiG (red), fAiG (green), iAFG (blue) and fAFG (purple). a) Antarctic ice volume (in 10^{15} m^3); b) Greenland ice volume (in 10^{15} m^3); c) southern sea-ice extent (in 10^{12} m^2); d) northern sea-ice extent (in 10^{12} m^2). A 10-year running mean has been applied to all time series.

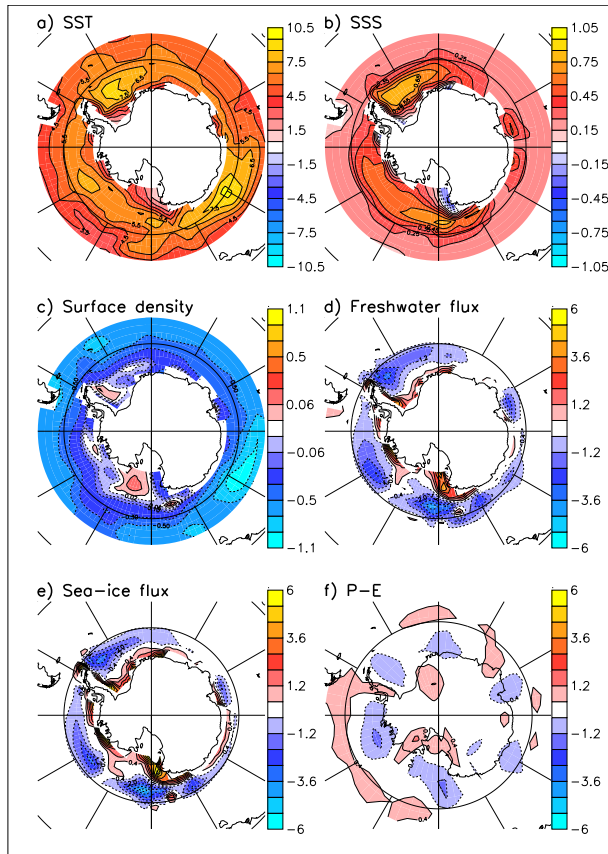


Figure 3. Difference between fAfG and CTRL averaged over years 2900 to 3000 of: a) Sea-Surface Temperature (SST) in K, b) Sea-Surface Salinity (SSS) in PSU, c) surface density in kg/m^3 , d) Total freshwater flux to the ocean (mm/day), e) sea-ice freshwater flux component (mm/day), f) Precipitation (P) minus Evaporation (E) component (mm/day). Increase in SST reduces surface density while increase in SSS enhances it. As a result of the compensation between increase in SST (a) and SSS (b), surface density diminishes in most of the Southern Ocean in fAfG compared to CTRL, but is increased regionally in the Weddell and Ross Seas (c). This regional increase in surface density associated with SSS augmentation deepens the mixed layer (not shown) and therefore explains the intensification of the AABW export observed in Figure 2.a. The increase in SSS is thus crucial and caused by changes in freshwater flux (d). The diminution of this flux actually spatially coincides with the SSS increase and is related, at the first order, to changes in sea-ice freshwater flux (e) and, at the second order, with P-E changes associated with the sea-ice cover retreat. When sea ice melts, the part of the ocean that was usually beneath is not isolated from the atmosphere anymore and new freshwater fluxes (P and E) apply and modify the forcing of this part of the ocean.

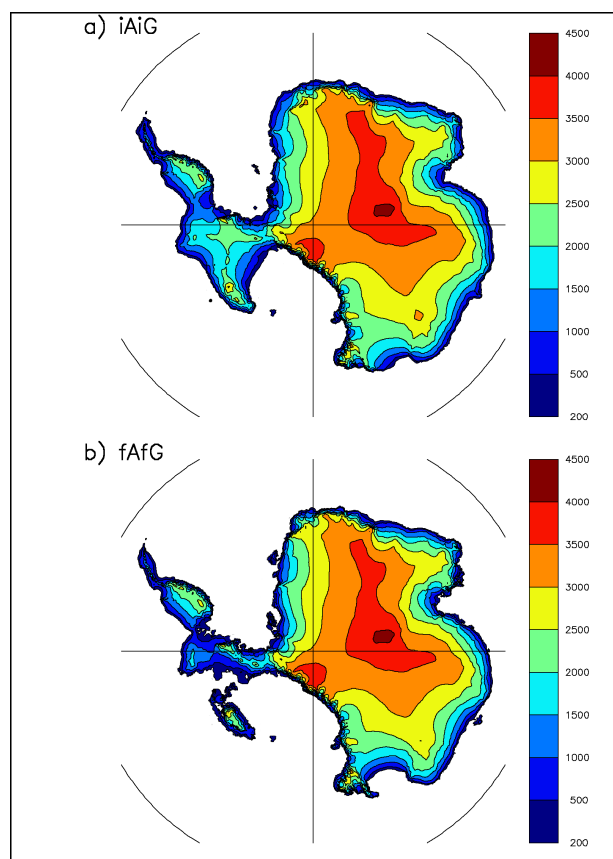


Figure 4. Ice-sheet surface elevation in Antarctica (in m) averaged over years 2900 to 3000. a) iAiG experiment. b) fAfG experiment. Note that, for fAfG, the melting is calculated but does not influence the other climate components that only see an ice sheet fixed to pre-industrial conditions.

	Antarctica	Greenland	Thermal expansion	Total
iAiG	3.2	8.0	2.6	13.8
fAfG	<i>10.0</i>	<i>3.4</i>	1.2	14.6
fAiG	<i>9.8</i>	7.9	1.5	19.2
iAfG	3.2	<i>3.6</i>	2.3	9.1

Table 1. Sea-level rise for the different experiments in comparison with CTRL after 3000 years (in m). Sea-level rise is decomposed into the contribution from Antarctic and Greenland ice sheets melting and thermal expansion. The figures in italic stand for the fact that they have been calculated, but the associated melting has not been released to the ocean and has therefore no impact on ocean circulation.